

## Kinetic Optimum of Volmer-Weber Growth

Vladimir M. Kaganer, Bernd Jenichen, Roman Shayduk, Wolfgang Braun, and Henning Riechert

*Paul-Drude-Institut für Festkörperelektronik, Hausvogteiplatz 5-7, D-10117 Berlin, Germany*

(Received 17 July 2008; revised manuscript received 27 November 2008; published 9 January 2009)

We find that the molecular beam epitaxy of Fe<sub>3</sub>Si on GaAs(001) observed by real-time x-ray diffraction begins by the abrupt formation of 3 monolayer (ML) high islands and approaches two-dimensional layer-by-layer growth at a thickness of 7 ML. A surface energy increase is confirmed by *ab initio* calculations and allows us to identify the growth as a strain-free Volmer-Weber transient. Kinetic Monte Carlo simulations incorporating this energy increase correctly reproduce the characteristic x-ray intensity oscillations found in the experiment. Simulations indicate an optimum growth rate for Volmer-Weber growth in between two limits, the appearance of trenches at slow growth and surface roughening at fast growth.

DOI: 10.1103/PhysRevLett.102.016103

PACS numbers: 81.15.Aa, 61.05.cp, 68.35.-p

The growth of crystalline films on substrates is classified by the same principles as wetting or nonwetting of liquids [1]. If the formation of the film surface and the film-substrate interface provides an energy gain  $\Delta\gamma < 0$  compared to the bare substrate surface, the film wets the substrate and grows layer-by-layer (Frank-van der Merwe growth). In the opposite case of an energy loss ( $\Delta\gamma > 0$ ), three-dimensional (3D) islands form, similar to liquid droplets with a finite contact angle (Volmer-Weber growth). Strained films may grow with 3D islands on top of the wetting layer to reduce the strain energy (Stranski-Krastanov growth).

Volmer-Weber growth is usually not desired for technological applications, and remains less studied. However, half of all material combinations (not considering interdiffusion and segregation) are of the nonwetting type, simply because the growth of a material *A* on *B* or that of *B* on *A* gives rise to opposite signs of  $\Delta\gamma$ . In addition, new device concepts demand increasingly dissimilar materials to be joined together on extremely small spatial scales. This requires the control of heterointerface formation on the mesoscopic and, ultimately, atomic scale. It is therefore very important to understand surface energy driven instabilities during interface formation.

Experimental investigations of metal heteroepitaxy often find two growth modes for the same system, with 2D growth at low temperatures and 3D growth at elevated temperatures [2–4]. However, the evolution of morphology and strain in these systems can be quite complex [5,6] and it becomes difficult to identify general mechanisms [7]. To explain the experiments, Markov and Kaischew [8] extended the original classification by Bauer [1] by introducing a supersaturation dependence of the energies of two-dimensional vs three-dimensional nuclei. This dependence was studied using mean-field rate equation models of growth [9] and Monte Carlo simulations [10]. Subsequent studies [11,12] have questioned this approach, arguing that higher supersaturation should rather affect the kinetics of deposition than the mode of nucleation, and

the mode of growth is not necessarily determined by the mode of nucleation.

In this Letter, we focus on an experimental system with negligible mismatch, avoiding the complications introduced by strain. This allows us to quantitatively study the generic case of surface energy driven Volmer-Weber growth. The growth oscillations found for this case have universal features that allow a straightforward identification in the experiment. They agree well with growth oscillations obtained from basic Monte Carlo simulations with just one additional parameter, describing the interface, added to the two common free parameters. These simulations predict a kinetic optimum for the growth of unstrained Volmer-Weber interfaces with minimum transient growth front roughening.

We grow Fe<sub>3</sub>Si films by molecular beam epitaxy (MBE) and simultaneously study the evolution of the system by grazing incidence x-ray diffraction in our MBE or diffractometer system at the wiggler beam line U125/2 KMC at the storage ring BESSY in Berlin [13]. The GaAs(001) templates are prepared in a separate III-V growth chamber and loaded via ultra high vacuum transfer. To obtain higher purity and stable cell operation, we stay below the melting point of the Si source. This results in a fairly low growth rate of 3 monolayers (ML) per hour that allows us to study the growth process *in vivo* with good time resolution. We use the standard definition of a monolayer as the single step height observed in atomic force microscopy and giving one x-ray intensity oscillation during growth. A monolayer of GaAs consists of two atomic layers, Ga and As, and is 0.28 nm thick. A monolayer of Fe<sub>3</sub>Si also consists of two atomic layers, one of them with iron only and the other containing both Fe and Si atoms, and has the same height.

Figure 1(a) shows the structure of Fe<sub>3</sub>Si on GaAs(001) we have determined in a previous post-growth surface x-ray diffraction study [14]. We have obtained the structure of the film, its termination at both interfaces, its exact thickness and relative position with respect to the substrate from fits to the crystal truncation rods (CTRs). In the

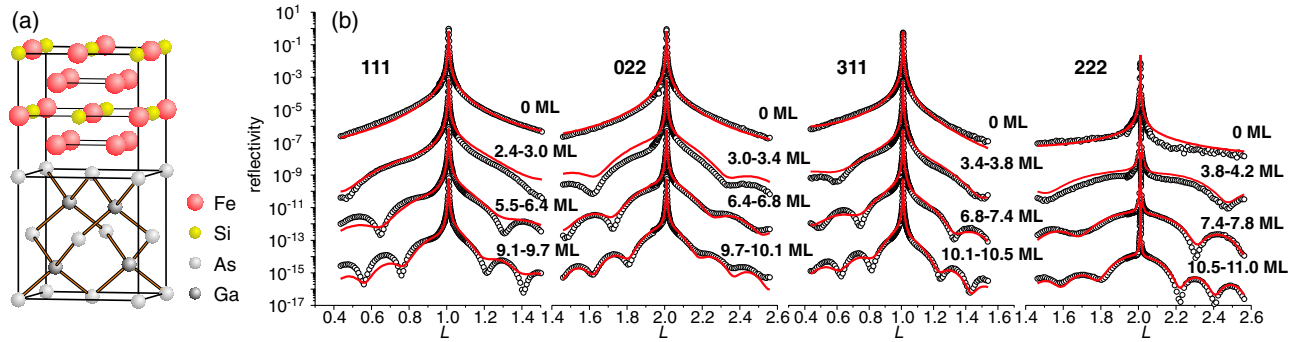


FIG. 1 (color online). (a) Epitaxy of  $\text{Fe}_3\text{Si}$  on  $\text{GaAs}(001)$  and (b) crystal truncation rods measured during growth (circles) with the fits assuming a complete coverage of the substrate by the film (lines). The substrate temperature is  $180^\circ\text{C}$ , the x-ray diffraction measurements are performed with an energy of 10 keV at a grazing incidence angle of  $0.3^\circ$ .

present work, we continuously measure the CTRs during growth. Figure 1(b) shows CTRs in the vicinity of different reflections. The reflections are measured in sequence, with one scan taking approximately 8 minutes (the deposition time of 0.4 ML). The CTR intensities are fitted by calculations using both multibeam dynamical and distorted wave Born approximations, as described in Refs. [14,15]. The thickness interference oscillations of the CTR intensity provide information on the thickness of the crystalline film during growth. Deposited atoms that are not yet incorporated in the crystalline lattice produce a minute contribution to the background.

The  $D0_3$  structure of  $\text{Fe}_3\text{Si}$  is characterized by two order parameters that describe the exchange of Si atoms with Fe atoms from two inequivalent sublattices [16,17]. A comparison of the different rods allows us to analyze the crystalline order of the film [14]. From the CTRs shown in Fig. 1(b), the measurements in the vicinity of the 022 reflection are not sensitive to disorder, while reflections 111 and 311 change with both order parameters. In the limiting case of a completely disordered structure, the thickness oscillations in the vicinity of the 022 reflection do not change, while for the 111 and 311 reflections, they disappear, leaving only the substrate peak. The 222 reflection is quasiforbidden in both GaAs and  $\text{Fe}_3\text{Si}$ , and the CTR intensity is strongly influenced by the adjacent allowed reflections. The  $22L$  CTR is therefore rather insensitive to the order in the sublattices. The measurements on different CTRs should indicate film thickness values that fall on a common curve. Such an agreement is reached with a  $\text{Fe}_3\text{Si}$  film that is fully ordered except for the top monolayer which is fully disordered.

The film thickness obtained from the CTR fringes, Fig. 1(b), is plotted in Fig. 2(a). After the deposition of 1 ML, crystalline  $\text{Fe}_3\text{Si}$  forms with a thickness just over 3 ML. Obviously, such a film can cover only part of the surface. This is in agreement with the fitted intensity curves in Fig. 1(b). Since the curves are properly scaled by adjusting the substrate maxima [14,15], the deficiency of the measured film intensity compared to the calculated

one implies incomplete coverage of the substrate by the film, Fig. 2(b). The film thickness becomes equal to the deposited amount of material only after deposition of about 7 ML. At the same thickness, the film density reaches the bulk value. Thus,  $\text{Fe}_3\text{Si}$  growth on GaAs begins by the formation of 3D islands at least 3 ML high.

The lateral sizes of the 3D islands are obtained from the lateral broadening of the CTRs. We measure the intensity profile across a rod by rotating the sample about its normal. The rod profiles obtained during growth, Fig. 3(a), agree well with a sum of two Lorentzians. We obtain the real-space size  $L$  of a surface feature from the corresponding full width at half maximum  $\Delta q$  of each peak in reciprocal space as  $L = 4/\Delta q$ . The narrow component represents a finite terrace size of approximately 100 nm that does not change during growth. The broad component is determined by the lateral sizes of the two-dimensional islands forming during growth. This island size increases from 2 to 8 nm, Fig. 3(b).

Figure 4 compares oscillations of the diffracted intensity during deposition of  $\text{Fe}_3\text{Si}$  and germanium on  $\text{GaAs}(001)$  at comparable growth rates. In both cases, the measurements are performed close to the bulk-forbidden reflections  $hk0$  (more precisely, at the reciprocal space points  $hkL$  with  $L = 0.04$ ) to provide maximum sensitivity to the surface morphology. Ge on GaAs serves as a reference example of Frank–van der Merwe growth, since both crys-

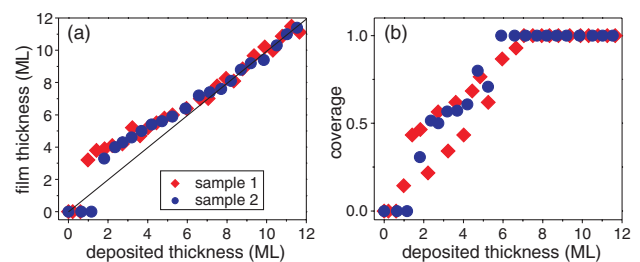


FIG. 2 (color online). (a)  $\text{Fe}_3\text{Si}$  epitaxial film thickness and (b) the fraction of the substrate covered by the film as obtained from the CTR measurements.

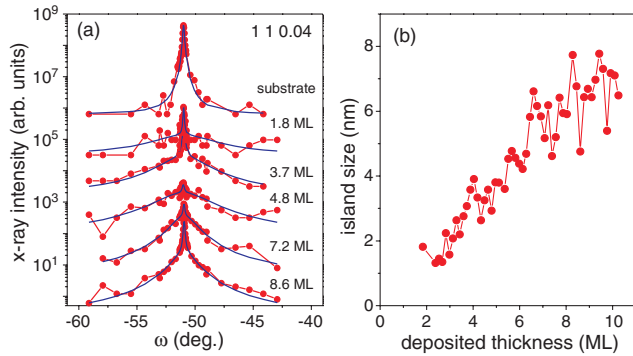


FIG. 3 (color online). (a) Diffraction peak profiles measured during epitaxial growth by rotating the sample about its normal through the reflection. The measured curves are fitted to a sum of two Lorentzians. (b) Lateral sizes of the 3D islands obtained from the broad component of the peak profile. The narrow component represents the constant average terrace width of 100 nm.

tals are structurally and energetically similar. The oscillations start immediately. In contrast,  $\text{Fe}_3\text{Si}$  growth begins with an initial plateau of low intensity. It is followed by several irregular oscillations with maxima shifted from the integer layer positions. These irregular oscillations are reproducibly the same on three samples grown under the same conditions. The regular layer-by-layer oscillations are established only after the deposition of 7–8 ML. After the sample is annealed at 300 °C, further growth oscillations are periodic from the very beginning. The unusual intensity oscillations are obviously a result of the formation of 3D islands during the initial  $\text{Fe}_3\text{Si}$  deposition on the bare substrate.

The transitional appearance of 3D islands may have either an energetic or a kinetic origin. Let us first discuss the energetics. The growth described above could be the result of a film thickness dependence of the energy gain  $\Delta\gamma$ . If  $\Delta\gamma$  decreased with increasing thickness, the film

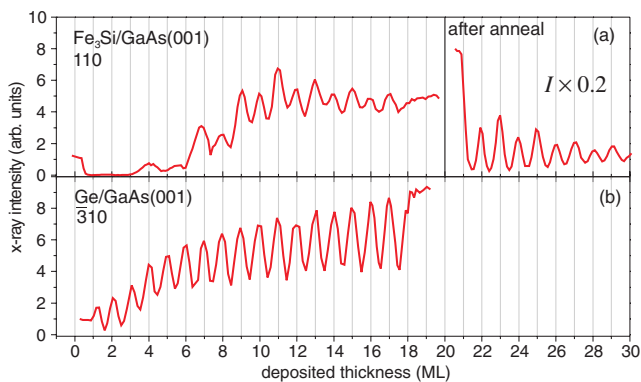


FIG. 4 (color online). Diffraction intensity oscillations during epitaxial growth of (a)  $\text{Fe}_3\text{Si}$  and (b) Ge on GaAs(001). In addition to the heteroepitaxy of  $\text{Fe}_3\text{Si}$  on the substrate, homoepitaxial growth after an anneal is shown for comparison.

surface and the interface would repel. Their interaction can be strong enough only for very thin films, which results in a smooth film when the thickness is large enough. The physical origin of such a repulsion could be the electronic confinement in very thin metallic films [18]. Such an effect is found, for example, during the growth of simple metals, lead and silver, on silicon or germanium surfaces at growth temperatures below 200 K [19–21] (for an overview and further references, see also Ref. [22]). Since we already know the atomic arrangement of  $\text{Fe}_3\text{Si}$  on GaAs(001) [14], we have performed *ab initio* calculations of the epitaxial system. We have used the generalized gradient approximation of density functional theory and the projector augmented-wave method with ultrasoft pseudopotentials implemented in the ABINIT program [23]. A kinetic energy cutoff of 18 Ha and a  $k$ -point set corresponding to  $6 \times 6$  points per surface Brillouin zone were used. We find a positive energy  $\Delta\gamma \approx 0.1 \text{ eV}/\text{\AA}^2$ , with a weak thickness dependence. Hence, the energy calculations indicate a Volmer-Weber growth mode; electronic confinement effects cannot explain the observed behavior.

We explore the growth kinetics by Monte Carlo simulations using a generic solid-on-solid model with simple cubic lattice [24]. To model Volmer-Weber growth, we make the bonds between film and substrate atoms weaker than the bonds within the film. In the standard model, the rate of an atomic jump is proportional to  $\exp(-E/kT)$ , where the energy  $E$  is calculated as  $E = E_S + nE_b$ . Here,  $n$  is the number of neighbors of a given atom before the jump,  $E_b$  is the bond energy, and  $E_S$  is the surface diffusion energy. The model involves only two independent parameters: one is the ratio  $E_b/kT$ , and the other is the ratio of the incident atomic flux  $F$  to the surface diffusion rate, proportional to  $\exp(-E_S/kT)$ . The choice of the values for these parameters does not qualitatively influence our results. We choose  $E_b = 0.2 \text{ eV}$  and  $E_S = 1.1 \text{ eV}$ . The first parameter yields compact islands at  $T = 500 \text{ K}$ , and the second one provides a reasonable nucleation distance for the deposition flux  $F = 1 \text{ ML}/20 \text{ min}$ .

The surface diffusion energy  $E_S$  represents the bonding to the underlying layer. We modify this energy for the first deposited layer only. In this way, the bonding of the film to the substrate becomes weaker than the bonding within the film. Thus, for the first deposited layer,  $E_S$  is replaced by  $E_S - \Delta E_S$ . The diffusion energy for the substrate material does not enter the simulations. Hence, the parameters involved in the *ab initio* calculations cannot be directly related to the surface energy gain  $\Delta\gamma$ .

The reduction of the surface diffusion barrier for the first layer drastically changes the initial growth compared to homoepitaxy, see Fig. 5(a). After the deposition of several monolayers, the substrate is not completely covered. Rather, 2–3 ML high islands form as a result of the favored upward jumps from the substrate to the film. Even after the deposition of 8 ML, trenches and pits down to the substrate

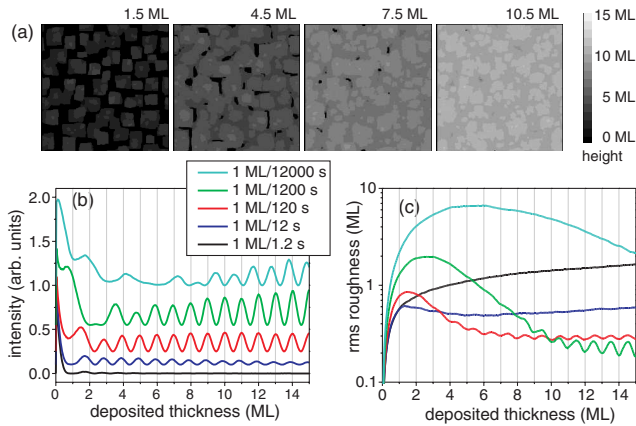


FIG. 5 (color online). Kinetic Monte Carlo simulations of Volmer-Weber growth: (a) snapshots at different depositions for the deposition rate  $F = 1/1200$  s (size of the simulation cell is  $200 \times 200$  atoms), (b) calculated intensity oscillations during deposition, and (c) time evolution of the root-mean-squared (rms) roughness. The simulations are performed with the same lowering of the surface diffusion barrier between substrate and film by  $\Delta E_S = 0.11$  eV.

persist. The film becomes continuous and smooth only after about 10 ML of deposition. Now, it continues to grow in an almost ideal layer-by-layer growth mode. Figure 5(b) shows the oscillating coherent intensities calculated from the kinetic Monte Carlo data. The curves are obtained for the antiphase condition by Fourier transforming  $\exp[i\pi h(x, y)]$ , where  $h(x, y)$  is the integer height at a given position. Hence, we do not take into account the difference in structure factors between film and substrate.

The intensity oscillations differ from the case of homoepitaxy and strongly depend on the growth rate. At the growth rate  $F = 1/1200$  s that is used to produce snapshots in Fig. 5(a), the intensity drops to zero after 2 ML deposition, then shows several irregular oscillations with shifted maxima, and only after about 7 ML deposition returns to the regular oscillations characteristic of layer-by-layer growth. This behavior agrees well with the experimental data of Fig. 4(a). When the growth rate is reduced and the system is closer to thermal equilibrium, larger surface features develop, but also deep trenches between them persist up to larger thicknesses. The regular growth oscillations are established after a longer delay. Note that in the case of the slowest simulated growth [the top curve in Fig. 5(b)], the oscillation maxima are not at integer positions even after 15 ML deposition. Such shifted maxima indicate that the film is yet not complete but has trenches down to the substrate. By increasing the growth rate, the formation of trenches and pits is reduced. The regular oscillations are established earlier, but have lower amplitude, since the surface is rougher.

The root-mean-squared (rms) roughness is larger for both fast and slow growth and smaller for intermediate growth rates, Fig. 5(c). A minimum roughness during

interface formation is achieved for the 1 ML/12 s growth rate and characterized by damped regular intensity oscillations with a small amplitude. Slower growth results in a larger initial roughness at the benefit of a smoother film at larger thickness. Thus, the common belief that the growth closer to thermal equilibrium gives rise to smoother films is not applicable to Volmer-Weber growth. In this case, the deposition needs to be sufficiently fast to avoid growth of three-dimensional islands, and slow enough to avoid kinetic roughening.

- [1] E. Bauer, *Z. Kristallogr.* **110**, 372 (1958).
- [2] W. A. Jesser and J. W. Matthews, *Philos. Mag.* **17**, 461 (1968).
- [3] C. T. Horng and R. W. Vook, *J. Vac. Sci. Technol.* **11**, 140 (1974).
- [4] R. W. Vook, C. T. Horng, and J. E. Macur, *J. Cryst. Growth* **31**, 353 (1975).
- [5] R. Koch, *J. Phys. Condens. Matter* **6**, 9519 (1994).
- [6] J. A. Floro, E. Chason, R. C. Cammarata, and D. J. Srolovitz, *MRS Bull.* **27**, 19 (2002).
- [7] M. T. Kief and W. F. Egelhoff, *Phys. Rev. B* **47**, 10785 (1993).
- [8] I. Markov and R. Kaischew, *Thin Solid Films* **32**, 163 (1976).
- [9] D. Kashchiev, *J. Cryst. Growth* **40**, 29 (1977).
- [10] D. Kashchiev, J. P. van der Eerden, and C. van Leeuwen, *J. Cryst. Growth* **40**, 47 (1977).
- [11] E. Bauer and J. H. van der Merwe, *Phys. Rev. B* **33**, 3657 (1986).
- [12] I. Markov and S. Stoyanov, *Contemp. Phys.* **28**, 267 (1987).
- [13] B. Jenichen, W. Braun, V. M. Kaganer, A. G. Shtukenberg, L. Däweritz, C.-G. Schulz, K. H. Ploog, and A. Erko, *Rev. Sci. Instrum.* **74**, 1267 (2003).
- [14] V. M. Kaganer, B. Jenichen, R. Shayduk, and W. Braun, *Phys. Rev. B* **77**, 125325 (2008).
- [15] V. M. Kaganer, *Phys. Rev. B* **75**, 245425 (2007).
- [16] V. Niculescu, K. Raj, J. I. Budnick, T. J. Burch, W. A. Hines, and A. H. Menotti, *Phys. Rev. B* **14**, 4160 (1976).
- [17] B. Jenichen, V. M. Kaganer, J. Herfort, D. K. Satapathy, H. P. Schönherr, W. Braun, and K. H. Ploog, *Phys. Rev. B* **72**, 075329 (2005).
- [18] Z. Zhang, Q. Niu, and C.-K. Shih, *Phys. Rev. Lett.* **80**, 5381 (1998).
- [19] H. Hong, C.-M. Wei, M. Y. Chou, Z. Wu, L. Basile, H. Chen, M. Holt, and T.-C. Chiang, *Phys. Rev. Lett.* **90**, 076104 (2003).
- [20] L. Floreano, D. Cvetko, F. Bruno, G. Bavdek, A. Cossaro, R. Gotter, A. Verdini, and A. Morgante, *Prog. Surf. Sci.* **72**, 135 (2003).
- [21] K. L. Man, Z. Q. Qiu, and M. S. Altman, *Phys. Rev. Lett.* **93**, 236104 (2004).
- [22] Z. Zhang, *Surf. Sci.* **571**, 1 (2004).
- [23] <http://www.abinit.org/>.
- [24] S. Clarke, M. R. Wilby, and D. D. Vvedensky, *Surf. Sci.* **255**, 91 (1991).